18th IMEKO TC10 Conference
“Measurement for Diagnostics, Optimisation and Control to Support Sustainability and Resilience”
Warsaw, Poland, September 26–27, 2022

Reliability estimation of Inertial Measurement units using Accelerated Life Test

Marco Carratù[1], Marcantonio Catelani[2], Lorenzo Ciani[2], Gabriele Patrizi[2], Antonio Pietrosanto[1], Paolo Sommella[1]

[1] Dept. of Industrial Engineering, University of Salerno, Via Giovanni Paolo II, 132, Fisciano, IT {mcarratu, apietrosanto, psommella}@unisa.it
[2] University of Florence, Dept. of Information Engineering, Via di S.Marta 3, 50139, Florence (IT) {marcantonio.catelani, lorenzo.ciani, gabriele.patrizi }@unifi.it

***Abstract* – In many different technological and industrial fields microelectronic device reliability is rising up as a fundamental aspect to consider during the design of diagnostic, optimization and control systems. Unexpected failures in diagnostic and control units could lead to a severe impact on the entire system/plant availability. Thus, reliability analysis must be carried out during the early phase of the design. MEMS (Micro-Electro-Mechanical Systems) based Inertial Measurement Units are widespread in diagnostic units to monitor acceleration, position and angular velocity of machinery. However, recent literature lack of a reliability estimation for this kind of devices. Thus, this paper proposes a measurement setup and a customized Accelerated Life Test plan for reliability estimation of a set of Inertial Measurement Units. A temperature-based stress test based on the HTOL (High Temperature Operating Life) protocol have been carried out to age the devices with the aim of obtaining a failure dataset. Results of the test have been used to predict device's reliability.**

Keywords – Arrhenius, Accelerometer; Gyroscope; Reliability; Testing; Industry, Innovation and Infrastructure.

I. INTRODUCTION

Inertial Measurement Units (IMUs) are common devices extensively used to easily and rapidly evaluate the positioning of a device. As a matter of fact, IMUs are multi-sensor measurement platforms used to monitor position, linear acceleration and angular velocity of an object toward X-axis, Y-axis and Z-axis [1], [2].

In many different industrial and technological fields, the above-mentioned data are becoming essential for diagnostic units, control systems and optimization algorithms. Some examples of such extensive expansions are self-driving vehicles, Unmanned Aerial Vehicles (UAV), wearable devices, robotic equipment and consumer electronics [3]–[5].

Micro-Electro-Mechanical Systems (MEMS) is the most cost-effective way to integrate small, accurate and stable IMUs within different kinds of systems. For this reason, it is becoming the leading technology in IMU's development overcoming the traditional piezoelectric devices [6]–[9].

One of the major concerns of MEMS-based IMU that is currently not significantly investigated in recent literature is their reliability metrics. The analysis of devices reliability for microelectronic components is a critical aspect that should be accurately investigated [10], [11]. Usually, reliability analysis of electric, electronic, and microelectronic components is carried out according to one of the following procedures:

- Reliability prediction using handbooks. This method represents a common and practical approach that allows designers to achieve a reasonable estimation of product failure rates according to failure data included in specific handbooks. In this case, the generic failure rate for every item is obtained according to the major technological characteristics and it is weighted considering several internal and external factors that influence the reliability performances of the devices [12]. The most common databases for electronic parts reliability prediction are the following:
    - MIL-HDBK 217F (last release is “Notice 2” published in 1995). This handbook is a milestone in reliability prediction developed for military purposes by the U.S. Department of Defence. It has been one of the most used handbooks in many different application fields [13].
    - Siemens SN29500 (last release published in 2013). This handbook is specifically developed for electric and electromechanical components [14].

- Handbook of 217 PLUS (2015). A generic handbook published to update the MIL-HDBK 217F database [15].
- Telcordia SR332 (last release is "Issue 4" published in 2016). This handbook includes one of the most updated databases for IoT and telecommunication applications [16].
- IEC 61709 (2017). This handbook published by the International Electrotechnical Commission contains the most recent dataset regarding electronic component reliability [17].

- Accelerated Life Test (ALT): this is an experimental approach used to evaluate the failure rate of a set of components accelerating the aging processes of the devices. This kind of tests are carried out forcing the items to endure severe conditions in terms of temperature, power supply, vibrations, and so on. These conditions must be above the nominal service operations in order to bring faults out in shorter time. The result of the test is a dataset containing a set of time-to-failure variables that could be used to implement a probabilistic life data analysis to obtain information regarding reliability, failure rate, probability density function, etc [18]–[20].

In case of MEMS-based inertial platform, a reliability prediction by means of handbooks is not feasible since this kind of components is not included in the major failure databases available in literature. Thus, this work introduces a preliminary test plan and measurement setup aimed at investigating the reliability of MEMS-based IMU under thermal conditions by means of an accelerated life test plan.

II. DEVICE UNDER TEST

The device taken into account in this work is a low-cost commercial 9-Dof (Degrees of freedom) MEMS-based inertial platform able to provide a 16-bit data output through SPI or I2C interfaces. Since it is a 9-Dof IMU, it integrates the following base sensors:

- Triaxial gyroscope used to measure the angular rate of an object according to X, Y, and Z directions. The device full scale is fully programmable up to ±2000 DPS (degrees per seconds).
- Triaxial accelerometer in order to measure the linear acceleration toward X, Y and Z axes. Also in this case the full scale is programmable, and it can reach values up to ±16 g.
- Triaxial magnetometer able to measure the static magnetic field toward X, Y, and Z-axis. The programmable full-scale reaches ±16 gauss.

Fig. 1. Picture of the devices under test mounted on a customized board.

The device under test also integrates an embedded temperature sensor that, according to the manufacturer, could be used to calibrate the device and compensate temperature drifts. A picture of the devices under test is illustrated in fig. 1, where a set of 25 devices are mounted on a customized electronic board.

III. DESCRIPTION OF THE TEST PLAN

The device under test is a quite common low-cost IMU which is currently integrated in several different application fields. In this work, the IMU under analysis is installed in a motorcycle for fault diagnosis purposes (for more information about the application, see [21]). Thus, the automotive field of application must be taken into account to customize the test plan.

The test procedure presented in this work can be classified as HTOL (High-Temperature Operating Life) Test Plan as described in the international standard IEC 60749-23:2004 [21] and in the testing procedure for solid-state technologies JESD22-A108F (2017) [22].

HTOL is a reliability test frequently applied to integrated circuits to determine their intrinsic reliability. HTOL forces the devices to endure high temperature, high voltage and dynamic operation for a predefined period of time. The DUT is usually monitored under stress and tested at intermediate intervals. Thus, HTOL is used to trigger potential failure modes and assess the device lifetime.

The severity of the presented HTOL test plan has also been tailored according to the automotive field of application, as in AEC-Q100-Rev-H (2014) [23]. Furthermore, the specifications of the considered devices have been considered to properly set the specific test requirements.

According to the normative reference cited above, the typical HTOL profile is performed exposing the devices at 125 °C for a minimum time of 1000 h. Furthermore, the standards recommend that the stress temperature may

exceed the operating temperature of the device, while remaining lower than the absolute maximum rated temperature indicated in the component data sheet.

According to the datasheets of the device under test, the maximum operating temperature is 85 °C while the absolute maximum storage temperature is 125 °C. Thus, tailoring the proposed HTOL on the considered device technology, the ambient temperature of the climatic chamber during the test shall be adjusted to ensure an operating temperature of 100 °C. The stress condition shall be applied continuously during the considered test duration. To determine the test duration, it is important to take into account that HTOL test duration is intended to meet or exceed an equivalent field lifetime under application use conditions. Since the temperature stress must be kept lower than the one suggested by the standardized HTOL procedure, then a higher time duration is required. Thus, a 6 months interval of exposition at 100 °C is proposed (approximately 4380 h).

For the sake of significance and effectiveness of the proposed test plan, a set of 25 identical devices is required to be tested. The devices are placed within a climatic chamber able to warm up and cool off the IMUs. To evaluate the functionalities of the devices during the test, the sensor's outputs are gathered together by dedicated multiplexers and then acquired by an ESP32 microcontroller located outside the chamber.

Several temperature test points have also been considered during the test, using thermocouples and RTDs (Resistance Temperature Detector) to acquire reference data.

A schematization of the measurement setup used for the proposed HTOL-based test plan is summarized in Fig. 2, highlighting the datalogger used for temperature measurement, the multiplexers, the microcontroller and a Personal Computer (PC) used for storage purposes.

Table 1. Summary of test requirements.

PARAMETER	VALUE
Test duration	6 months
Exposition temperature	100 °C
Number of devices	25
Normative reference	HTOL

A summary of the test severity is reported in Table 1, emphasizing the test duration, the exposition temperature, the number od devices under test and the normative reference.

IV. ACCELERATION MODEL

In this section the results of the results of the proposed HTOL procedure are discussed. An exposition time of 6 months at 100 °C results in a longer ageing of the device according to the Arrhenius degradation model. The latter can be used to describe the aging rate of a device in case of accelerated test procedures by means of the acceleration factor A_f defined as follow [19]:

$$A_f = \exp\left[\frac{E_a}{K_B}\left(\frac{1}{T_{op}} - \frac{1}{T_{test}}\right)\right] \quad (1)$$

Where E_a (expressed in eV) is a parameter called activation energy used to dscribed the energy required to trigger the failure mechanisms, $K_B = 8.617 \cdot 10^{-5} \frac{eV}{K}$ is the Boltzmann's constant, while T_{op} and T_{test} are the operating temperature and the test temperature, respectively.

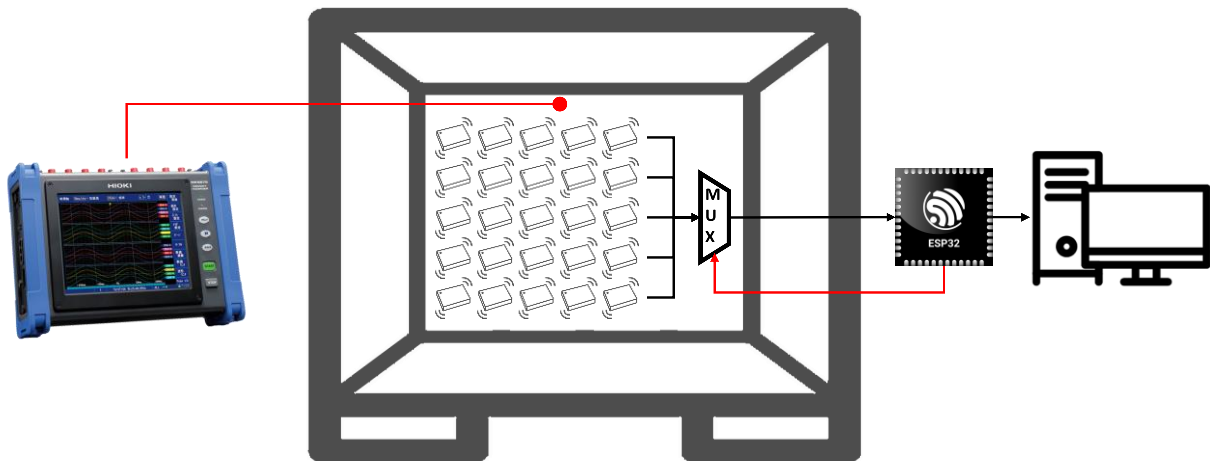

Fig. 2. Schematization of the measurement setup for the reliability testing of the Inertial platform under analysis including 25 boards, a datalogger, a thermal camera, some multiplexers, an esp32 microcontroller and a PC.

The relationship in eq. (1) stands for the acceleration given by the high temperature during the test to the aging of the devices. Thus, it represents how quickly a device ages when used at temperature T_{test} instead of using it at standard operating condition T_{op}.

As a consequence, the following relathionship can be derived:

$$\tau_{T_{op}} = A_f \cdot \tau \quad (2)$$

Where τ represents the test duration, while $\tau_{T_{op}}$ stands for the equivalent test time at the operating temperature T_{op} derived using the acceleration factor in eq. (1).

Considering a protected environment of installation for the IMU under analysis, the operating temperature could be set equal to $T_{op} = 30\ °C$, while the test temperature is $T_{test} = 100\ °C$ according to section III.

Regarding the activation energy, this parameter is of foundamental importance in the evaluation of the accelerating factor. However, in many cases for electronic devices is difficult to precisely estimathe the correct value. In this work, a systematic literature review has been carried out to estimate the optimal value of the activation energy E_a. There are only few works in literature that estimate an activation energy for MEMS-based IMU. The main results are summarized in Table 2 along with the relative acceleration factor calculated through eq. (1), the equivalent test time evaluated using eq. (2) and the bibliographic reference.

The table summarizes the results considering four different activation energy values found in literature. Furthermore, it also includes a final row evaluated using the average activation energy betwen the previous values. The average value represents a more accuare estimation of the E_a parameter giving more trustworthy results.

In this scenario, considering $E_a = 0.63\ eV$ and taking into account eq. (1)-(2), 6 months of test procedure carried out at temperature $T_{test} = 100\ °C$ are equivalent to 405575 h of aging at ambient temperature (i.e., 30 °C). This means that the test procedure described in section III led to over 46 years of aging of the IMUs.

Table 2. Summary of literature review for the activation energy MEMS-based IMU.

ACTIVATION ENERGY E_a	ACCELERATION FACTOR A_f	EQUIVALENT TEST TIME $\tau_{T_{op}}$	REFERENCE
0.7 eV	153.1467	670783 h	[24]
0.58 eV	64.6424	283134 h	[25]
0.81 eV	337.6616	1478958 h	[26]
0.42 eV	20.4675	89648 h	[27]
0.63 eV	**92.5970**	**405575 h**	**Average value**

V. ANALYSIS OF THE RESULTS

As described in Table 1, 25 identical devices have been tested using the setup illustarted in Fig. 2. Despite the temperature overstress applied for 6 months, the 25 devices experienced no failures during the test. The final inspection after the aging test led to positive results, confirming the correct functioning of all the IMUs.

However, an interesting phenomenon have been observed analyzing the data acquired by the IMUs during the test. In particular, the output of the accelerometers, gyroscopes and magnetometers highlight some parameter difts for every considered axis and every considered device. For the sake of brevity, only the output of one random sensor are illustrated in the following. In particular, Fig. 3 shows the output of the accelerometed integrated within IMU #22 during the test. Similarly, Fig. 4 illustrates the data acquired by the gyroscope of IMU #3 toward X, Y and Z axis, while Fig. 5 shows the magnetomer's output during the test.

Analyzing the acquired data, the following considerations can be drawn:

- All the accelerometers follow the trends shown in Fig. 3. The output of the sensors toward Z-axis expirienced a significant increase of the output variability during the test, along with a minor decrease of the mean value of the acquired gravitational acceleration. Instead, considering X and Y axes, both phenomena have a minor magnitude.
- Almost all gyroscopes under test follow the degradation behavior shown in Fig. 4. In contrast to the accelerometers, in this case the Z axis represents the output characterized by the lower data variability during the entire test. All the axis experienced the same degradation, which consistes of a significant drift of the average value acquired by the sensor. For all the gyroscopes, the drifts could be either negative or positive.
- Similar to the gyroscopes, also the magnetometers (Fig. 5) shown a drift of the average acquired value during time that could be eithe rnegative or positive, depending on the axis and the device considered.

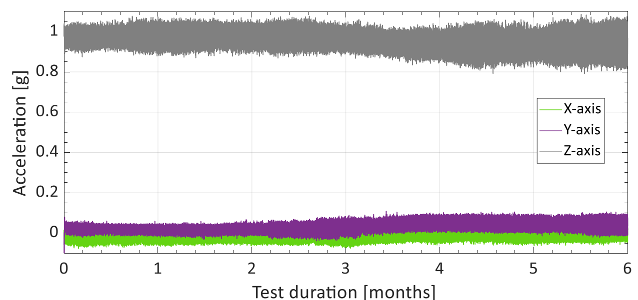

Fig. 3. Analysis of accelerometer output toward X, Y and Z axis during the entire test. IMU #22 is involved.

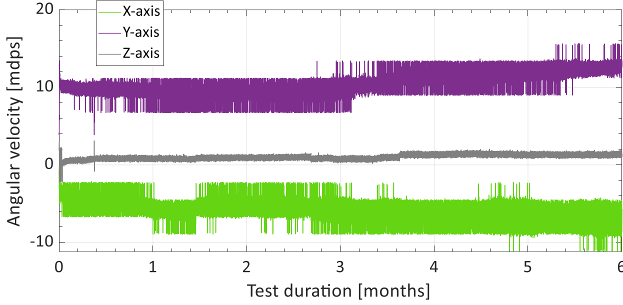

Fig. 4. Analysis of gyroscope output toward X, Y and Z axis during the entire test. IMU #3 is involved.

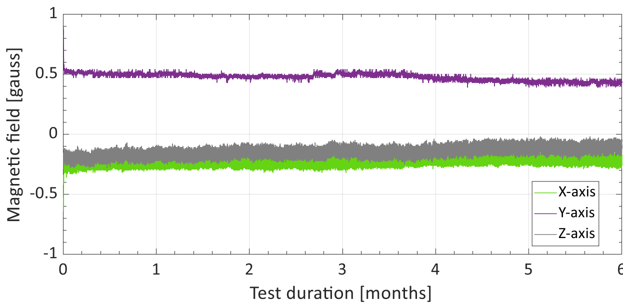

Fig. 5. Analysis of magnetometer output toward X, Y and Z axis during the entire test. IMU #15 is involved.

The major impact of the aging test performed on the 25 devices under analysis is a decrease of the measurement accuracy due to the increase of the output variability and the variation of the average acquired value in static conditions. Since no failure mechanisms have been triggered during the test, it is not possible to perform a life data analysis to estimate the failure rate and the system reliability according to a specific failure distribution (such as exponential, Weibull, lognormal, etc.). However, when a test ends after a certain time τ with none of the N devices having failed, it is possible to estimate the failure rate of the population using the Chi-squared distribution and assuming a constant failure rate [28]. More in detail, it is necessary to define the cumulative test time τ_{cum} as the total test duration endured by the entire population:

$$\tau_{\mathrm{cum}} = \mathrm{N} \cdot \tau_{\mathrm{T_{op}}} = \mathrm{N} \cdot \mathrm{A_f} \cdot \tau \tag{3}$$

Thus, an upper $(1-\alpha)\,\%$ confidence limit for the device failure rate λ_{IMU} could be evaluated as follow:

$$\widehat{\lambda_{IMU}}\Big|_{1-\alpha} = \frac{\chi^2[2, 1-\alpha]}{2 \cdot \mathrm{N} \cdot \mathrm{A_f} \cdot \tau} = \frac{\chi^2[2, 1-\alpha]}{2 \cdot \tau_{\mathrm{cum}}} \tag{4}$$

The results of the estimated failure rate for the IMU under test $\widehat{\lambda_{IMU}}\Big|_{1-\alpha}$ considering different confidence interval are summarized in table 3.

Table 3. Failure rate estimated using Chi-squared distribution with different confidence intervals.

Confidence interval	**α**	**Estimated failure rate**
50%	0.5	68.4 FIT
80%	0.2	158.7 FIT
90%	0.1	227.1 FIT
95%	0.05	295.5 FIT
99%	0.01	454.2 FIT

All the results reported in Table 3 are evaluated considering an activation energy of $\mathrm{E_a} = 0.63$ eV (i.e., average value in Table 2) and thus an acceleration factor of $A_f = 92.597$. The estimated failure rate is expressed using the FIT (Failure In Time) unit of measurement, which correspond to failure over 1 billion hours.

VI. CONCLUSIONS

In this work, a customised test plan and a measurement setup for the reliability estimation of MEMS-based IMU have been implemented. A temperature-based stress test based on the HTOL protocol have been carried out to age the devices with the aim of obtaining a failure dataset. However, the devices under test experienced no failure mechanisms during the proposed aging procedure. The test led to a decrease of the measurement accuracy for all the 25 IMUs due to the increase of the output variability and the variation of the average acquired value in static conditions. Since no failure have been discovered, an upper $(1-\alpha)\,\%$ confidence limit for the device failure rate have been proposed using the Chi-squared distribution. The results prove the outstanding performances in terms of reliability requirements for the considered IMU which successfully survived to an equivalent aging of over 46 years.

REFERENCES

[1] D. Capriglione *et al.*, "Characterization of Inertial Measurement Units under Environmental Stress Screening," in *2020 IEEE International Instrumentation and Measurement Technology Conference (I2MTC)*, 25-28 May 2020, Dubrovnik, Croatia.

[2] B. Altinoz and D. Unsal, "Determining efficient temperature test points for IMU calibration," in *2018 IEEE/ION Position, Location and Navigation Symposium (PLANS)*, 23-26 Apr. 2018, Monterey, CA, USA, pp. 552–556.

[3] Y. Weizman, O. Tirosh, F. K. Fuss, A. M. Tan, and E. Rutz, "Recent State of Wearable IMU Sensors Use in People Living with Spasticity: A Systematic Review," *Sensors*, vol. 22, no. 5, p. 1791,

2022.

[4] D. Capriglione *et al.*, "Experimental Analysis of Filtering Algorithms for IMU-Based Applications Under Vibrations," *IEEE Trans. Instrum. Meas.*, vol. 70, Article Sequence Number: 3507410, 2021.

[5] A. Ochoa-de-Eribe-Landaberea, L. Zamora-Cadenas, O. Peñagaricano-Muñoa, and I. Velez, "UWB and IMU-Based UAV's Assistance System for Autonomous Landing on a Platform," *Sensors*, vol. 22, no. 6, p. 2347, 2022.

[6] J. Otegui, A. Bahillo, I. Lopetegi, and L. E. Diez, "Evaluation of Experimental GNSS and 10-DOF MEMS IMU Measurements for Train Positioning," *IEEE Trans. Instrum. Meas.*, vol. 68, no. 1, pp. 269–279, Jan. 2019.

[7] U. Qureshi and F. Golnaraghi, "An Algorithm for the In-Field Calibration of a MEMS IMU," *IEEE Sens. J.*, vol. 17, no. 22, pp. 7479–7486, Nov. 2017.

[8] A. Schiavi, A. Prato, F. Mazzoleni, G. D'Emilia, A. Gaspari, and E. Natale, "Calibration of digital 3-axis MEMS accelerometers: A double-blind «multi-bilateral» comparison," in *2020 IEEE International Workshop on Metrology for Industry 4.0 & IoT*, 3-5 Jun. 2020, Roma, Italy, pp. 542–547.

[9] G. D'Emilia and E. Natale, "Network of MEMS sensors for condition monitoring of industrial systems: Accuracy assessment of features used for diagnosis," in *17th IMEKO TC 10 and EUROLAB Virtual Conference "Global Trends in Testing, Diagnostics & Inspection for 2030"* 20-22 October 2020, Virtual conference, pp. 356–361.

[10] J. Iannacci, "Reliability of MEMS: A perspective on failure mechanisms, improvement solutions and best practices at development level," *Displays*, vol. 37, pp. 62–71, Apr. 2015.

[11] A. Ahari, A. Viehl, O. Bringmann, and W. Rosenstiel, "Mission profile-based assessment of semiconductor technologies for automotive applications," *Microelectron. Reliab.*, vol. 91, pp. 129–138, Dec. 2018.

[12] M. Catelani, L. Ciani, A. Bartolini, G. Guidi, and G. Patrizi, "Standby Redundancy for Reliability Improvement of Wireless Sensor Network," in *2019 IEEE 5th International forum on Research and Technology for Society and Industry (RTSI)*, 9-12 Sep. 2019, Florence, Italy, pp. 364–369.

[13] MIL-HDBK-217F, "Military Handbook - Reliability Prediction of Electronic Equipment." US Department of Defense, Washington DC, 1991.

[14] SN 29500, "Failure rates of components." Siemens, 2013.

[15] HDBK-217Plus, "Handbook of 217Plus - Reliability Prediction Models." Quanterion Solutions Incorporated, 2015.

[16] Telcordia SR-332, "Reliability Prediction Procedure for Electronic Equipment," no. 4. Telcordia Network Infrastructure Solutions (NIS), 2016.

[17] IEC 61709, "Electric components - Reliability - Reference conditions for failure ratesù and stress models for conversion." International Electrotechnical Commission, 2017.

[18] M. Catelani, L. Ciani, G. Guidi, and G. Patrizi, "Accelerated Testing and Reliability estimation of electronic boards for automotive applications," in *2021 IEEE International Workshop on Metrology for Automotive (MetroAutomotive)*, 1-2 Jul. 2021, Bologna, Italy, pp. 199–204.

[19] L. A. Escobar and W. Q. Meeker, "A Review of Accelerated Test Models," *Stat. Sci.*, vol. 21, no. 4, pp. 552–577, Nov. 2006.

[20] M. R. Piña-Monarrez, "Weibull analysis for normal/accelerated and fatigue random vibration test," *Qual. Reliab. Eng. Int.*, vol. 35, no. 7, pp. 2408–2428, Nov. 2019.

[21] IEC 60749-23, "Semiconductor devices - Mechanical and climatic test methods – Part 23: High temperature operating life." International Electrotechnical Commission, 2004.

[22] JEDEC Solid State Technology, "JEDEC Standard - Temperature, Bias, and Operating Life." JESD22-A108F, 2017.

[23] Automotive Electronics Council, "Failure Mechanism Based Stress Test Qualification for Integrated Circuit." AEC - Q100 - Rev-H, 2014.

[24] Analog Devices, "Reliability Data." https://www.analog.com/en/about-adi/quality-reliability/reliability-data/wafer-fabrication-data.html (accessed Jun. 14, 2022).

[25] Automotive Electronics Council, "Failure mechanism based stress test qualification for optoelectronic semiconductors in automotive applications." AEC - Q102 - Rev A, 202AD.

[26] W. M. van Spengen, R. Puers, R. Mertens, and I. De Wolf, "A comprehensive model to predict the charging and reliability of capacitive RF MEMS switches," *J. Micromechanics Microengineering*, vol. 14, no. 4, pp. 514–521, Apr. 2004.

[27] G. J. Papaioannou *et al.*, "Effect of space charge polarization in radio frequency microelectromechanical system capacitive switch dielectric charging," *Appl. Phys. Lett.*, vol. 89, no. 10, p. 103512, Sep. 2006.

[28] A. Birolini, *Reliability Engineering*. Berlin, Heidelberg: Springer Berlin Heidelberg, 2017.